Journal of Engineering Science and Technology
Vol. 17, No. 6 (2022) 3926 - 3939

SILK FIBER ORIENTATION EFFECT ON FLEXURAL AND TENSILE STRENGTH OF ZEOLITE-REINFORCED HIGH-DENSITY POLYETHYLENE COMPOSITES

PURNOMO[1,*], PUTU H. SETYARINI[2],
HELMY PURWANTO[3], SOLECHAN[1]

[1]Mechanical Engineering Department, Universitas Muhammadiyah Semarang, Jalan Kedungmundu Raya No. 18 Semarang, Indonesia
[2]Mechanical Engineering Department, Brawijaya University, Jalan Veteran, Malang, Indonesia
[3]Mechanical Engineering Department, Universitas Wahid Hasyim, Jalan Menoreh Tengah X/22 Sampangan, Semarang, Indonesia
*Corresponding Author: purnomo@unimus.ac.id

Abstract

The role of silk fibers (SF) orientation is very decisive on the mechanical performance of high-density polyethylene (HDPE) with zeolite (Z) as a reinforcement material. This work aims to analyse the tensile and flexural characteristics of zeolite-filled HDPE (Z/HDPE) composites due to the incorporation of SF in numerous orientations. The SFs with a length of approximately 1 mm is chopped off for incorporation in the powder dry mix of Z and HDPE, which is ready for SF-oriented mold at angles ranging 0°, ±22.5°, ±45°, ±67.5°, and ±90°. The compression moulding technology creates composites to fit dumbbell shapes. The flexural test was carried out in compliance with the ASTM D790 standard, whereas tensile properties including elastic modulus, tensile strength, elongation at break as well as yield strength were assessed on dumbbell shape composites. The findings demonstrate that the maximum force, as well as the elastic modulus, drop by changing the orientation of the fiber towards 0°. This propensity also takes place in failure and energy-breaking strains. Flexural strength and breaking energy decreased by about 5-10% of the initial value for each additional 22.5° fiber orientation angle. However, the flexural modulus and other tensile properties are decreased irregularly by the addition of the fiber orientation angle. Furthermore, the theoretical E-modulus value exceeds the experimental value by about 15 to 20%. The flexural and tensile strength of the composite is maximum at the SF orientation angle of 0°.

Keywords: Flexural, HDPE, Silk fiber, Tensile, Zeolite.

1. Introduction

Given that it is biocompatible, low price, and abundant in availability, biomaterials from natural fibers attracted a lot of interest from researchers. Both the flexural modulus and E-modulus of natural fiber are relatively much stronger than synthetic ones [1-3]. Moreover, they are low, abrasive, and well biodegraded [4-6]. The direction of the reinforcement materials strongly influences the mechanical performance of composite materials. Consequently, it is significant to systematically examine the artificial composites and the impact of fiber orientation. In particular, the tensile strength, elastic modulus, and chemical properties such as corrosion resistance are promoted by reinforcement of ductile polymers incorporated fibers. Various fiber forms including glass, carbon, and aramid, are often used in thermoplastic matrices as reinforcement [7], but they get drawbacks like high production costs and are hard to recycle [8]. Natural fibers have extensively been used to strengthen polymer matrices in different engineering materials to consider the achievement of strong final mechanical properties.

Composites with thermoplastic matrices reinforced with fibers have been conducted with a specific focus on the orientation of fibers in composites. Different composite moulding techniques can be applied, including injection moulding, wet lay, extruder, and pultrusion, but in those techniques, the fiber orientation cannot be controlled. Compression moulding is the best method relative to those referred to produce those composites [9-12].

SF is a fiber dependent on a protein made from arthropods, including silkworms and spiders [13, 14]. The SF offers desirable properties, including strong elongation and low density [15, 16]. In some instances, also SFs show imminent glass fibers mechanical properties [17, 18]. SF is also ideal for different engineering applications as replacements for glass fibers [18-20]. SF is now commonly developed for biomedical applications, particularly bone graft technology, for human bone regeneration due to their biocompatibility and osteoconductivity [21-25].

This study aims to improve mechanical performance by integrating SF in different orientations within Z/HDPE composites. This is in line with an earlier study by Purnomo and his co-workers [26-29]. The chopped SF was applied as reinforcement at numerous orientation angles. Compression forming processes are used in the production process of SF-reinforced Z/HDPE composites. Impact on the tensile strength and flexural strength for various SF orientation angles was assessed. There were also discussed theoretical and experimental E-modulus.

2. Materials and Methods

2.1. Materials

Silkworm SF, natural mordenite zeolite, and HDPE (injection grade) are the materials component of this study. Zeolite, as well as HDPE, are turned into powder. Chopped SF around 1 mm long was introduced to the calcinated Z/HDPE powder dry mixture. The composition of chopped SF towards the powder mixture of Z/HDPE is 2 wt.%.

2.2. Manufacturing Procedure

Chopped SFs were positioned at the track of path length center and dispersed uniformly over the entire sample in an arrangement of 0°, ±22.5°, ±45°, ±67.5°, and

±90° as shown in Fig. 1. In order to keep the fiber orientation maintained at the required angle, the fibers are first laid out on one half of the matrix, after all the fibers are oriented as required, the other half of the matrix is poured on top. This process is placed at the bottom of the mold. The press will then be closed, the top and bottom of the mold are given heat treatment around 122°C, and the pressure is set from the top path of approximately 3,447 kPa with a holding time of 4 min in order to longevity, and indissolubleness. Samples were annealed at 80°C for 24 hrs on atmospheric pressure. The manufacturing process is schematically shown in Fig. 2.

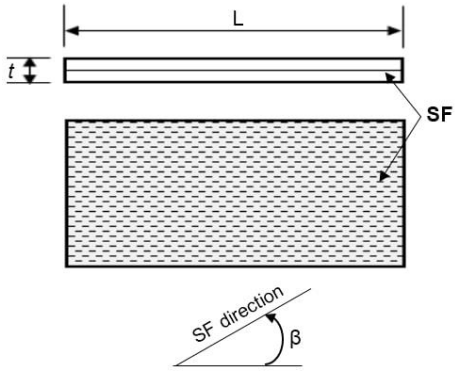

Fig. 1. A structural representation for 0° SF-reinforced Z-HDPE composites with a front and top view. The β is SF angle, L is composite length, and t is composite width.

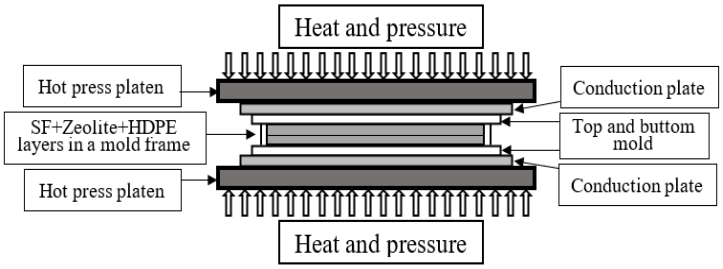

Fig. 2. Schematic representation of the hot press to fabricate composites.

2.3. Mechanical Testing

In terms of achieving the flexure properties, including flexural strength and flexural modulus, flexural tests have been performed in a three-point bending test, suggested by ASTM D790, in a 32 span/depth ratio. According to ISO 527, the test is conducted on a universal testing machine (WDW-20E) by applying a tensile force to a dumbbell-shaped (Fig. 3) and measuring the tensile properties of the specimen material under stress. The test was conducted at a 3 mm/min test speed until the specimen breaks. About 25°C of ambient temperature was preserved. The stress-strain curves obtained indicated the tensile properties including E-modulus, tensile strength, and break-up elongation. E-modulus from the experiment is contrasted with the theoretical. All mechanical test were carried out on composites

with fiber orientation variations of 0, ±22.5, ±45, ±67.5, and ±90. Each fiber orientation was tested by 5 samples.

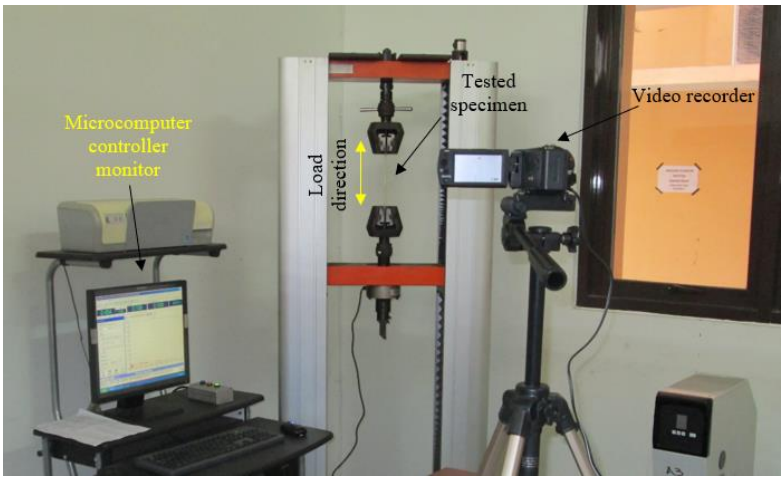

Fig. 3. Test set-up of composite tensile test.

2.4. Fracture Surface Characterization

Scanning electron microscopy (SEM) employs to investigate the tensile fracture surface of the tested sample. Before the observation, the gold/palladium coating was applied to the surface samples.

3. Results and Discussion

3.1. Flexural properties

In SF various orientations, the flexural strength is presented in Fig. 4(a). It was shown that their value reduces as the SF angle rises. The FS is decreased by 38% (90°) from 268 MPa at the angle of 0° SF. The flexural modulus is similarly inclined to flexural strength, Fig. 4(b). The orientation of the fibers on the material's longitudinal direction suggests greater flexural characteristics than another, which have shifted beyond 0° in fiber orientation.

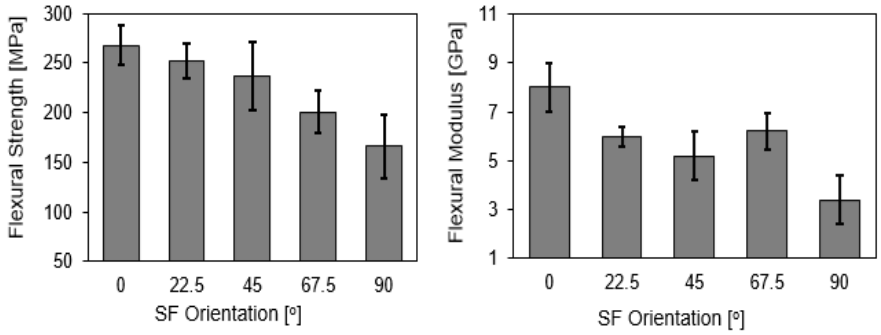

(a) flexural strength **(b) flexural modulus**

Fig. 4. The profiles for flexural properties for various SF orientation.

The SF-orientated composites are the most flexural effective in the longitudinal direction. On the contrary, it moves the flexural properties from the longitudinal direction. These findings demonstrate that the orientation of the fibers greatly impacts the flexural properties [30, 31].

The results of this laboratory test are consistent with those of several other studies [32, 33] that show that fiber reinforcement increases flexural strength significantly, particularly when the fibers are oriented parallel to the length of the specimen or perpendicular to the loading (0°). According to Van Heuman et al. [34] review article, the orientation of the reinforced fiber is more important than the type of fiber used in strengthening the flexural strength of the fiber-reinforced composites. Changes in fiber orientation had no effect on transverse strength.

3.2. Tensile properties

Figure 5(a) shows the strain at break, while the breaking energy is shown in Fig. 5(b). The greatest stress and energy breaking were achieved in the longitudinal direction (0°) instead of orientation over 0°.

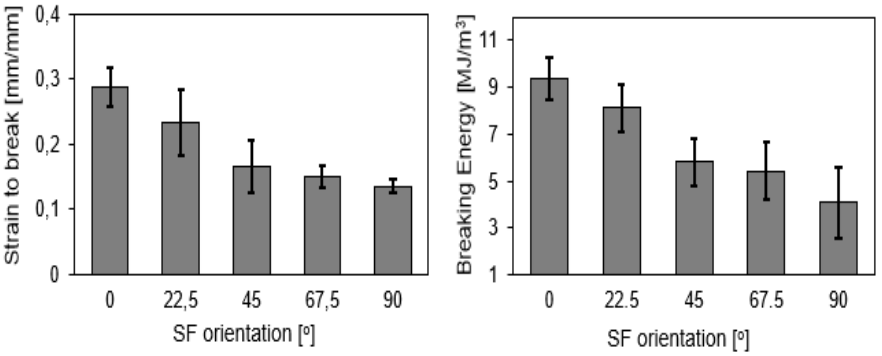

(a) Strain to break for various SF orientation angels

(b) Breaking energy for various SF orientation angels

Fig. 5. The relationship of fiber orientation to strain at failure (a), and energy breaking.

The ultimate tensile strength and E-modulus for dumbbells shape tested versus SF orientation are depicted in Fig. 6. The SF orientation effectively ensures the tensile strength to decline, Fig. 6(a) and the composite E-modulus, Fig. 6(b). The tensile strength enhances when SF is parallel to specimen length and tensile force direction. This was also possible with composite E-modulus and composites with a 22.5° angle of inclination. The result is an efficient force redeployment on the 0° SF-Z/HDPE composite interface. It represents the previous studies reported by many researchers [35-37], albeit on different materials.

This phenomenon can be explained that the direction of loading can be used as a reference in the preparation of reinforcing fibers. Slightly the angle of the fiber shifts from the direction of the load, the tensile properties including strain to break, breaking energy, ultimate tensile strength, and E-modulus of the material weaken substantially. However, the joining of fibers is very advantageous because it can increase the tensile properties of the composite as long as the direction of the fibers is arranged parallel

to the direction of the force, even a slight shift at ±22.5° is still better than without the fiber. This anisotropic behavior indicates that the incorporation of fiber is less favourable if the fiber direction exceeds ±22.5° from the loading direction.

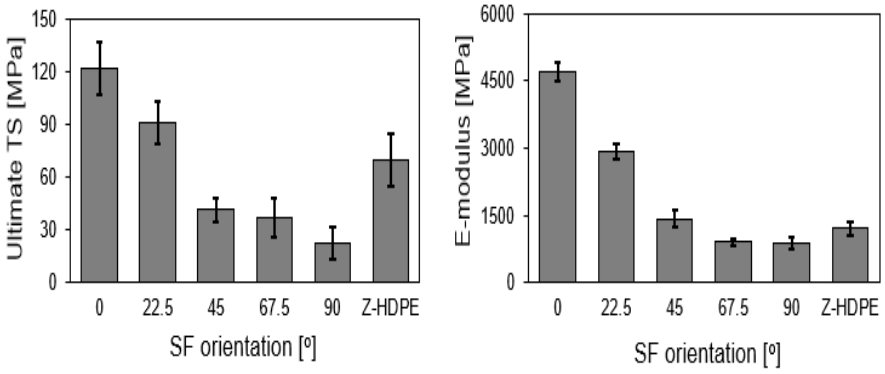

(a) Ultimate tensile strength (UTS) of composites

(b) E-modulus of composites

Fig. 6. Composites tensile properties versus SF orientation.

Typical elongation at break throughout the various SF orientations the samples tested was shown in Fig. 7. It is clearly shown that the extension during the break improves by raising the angle of the SF to 45°, and over that angle, with an orienting angle of 90°, falls to its least level. In general, the addition of 45° SF reduces the strain so that it is closer to the strain value of the fiber-free composite. In addition, this strain phenomenon at 45° orientation is similar to the results of previous studies even though the studied material is different [38, 39].

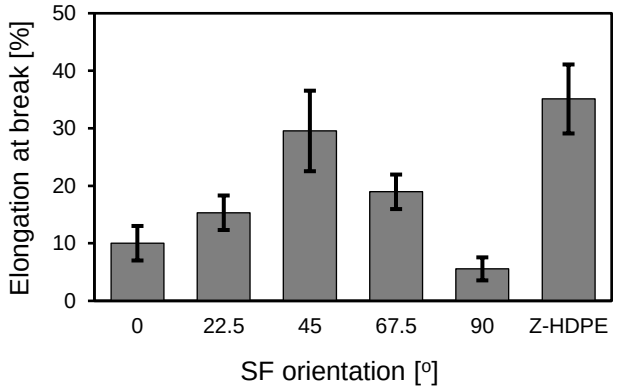

Fig. 7. Elongation profile for the sample tested in different SF orientation.

The rule-of-mixture principle can be used to study of the E-modulus in composites tested. The key assumption is that the fiber and matrix are similarly stressed by the effects of the load on the fiber path in the traditional rule of the mix. Furthermore, the matrix fiber interface is expected to be preferably adhesive, with

fibers well dispersed throughout the host polymer matrix. The fibers are called compatible. The modulus of composite (E_c) can be expressed [40]:

$$E_c = V_f . E_f + V_m . E_m \tag{1}$$

E-modulus and volume fraction of fibers was denoted by E_f and V_f, respectively, while the matrix parameters related to the E-modulus and volume fraction was represented by E_m and V_m, respectively. Several studies successfully alter Eq. (1) by fiber specification modification in the fiber area to four emendations [40]. Their parameters modified are fiber diameter distribution, fiber length distribution, and the ratio of the fiber indicated by κ, η_d, η_1, and η_0, respectively. Equation (1) was adapted successfully to Cording et al. [41]. The new formula is therefore presented in the new equation version [40, 41]:

$$E_c = \kappa \eta_d \, \eta_1 \eta_0 V_f \, E_f + V_m \, E_m \tag{2}$$

The proportion factor of fiber, η_0, can be defined in the equation, as Krencel states [39]:

$$\eta_0 = \sum_n a_n \cos^4 \theta_n \tag{3}$$

The α_n function is the fiber fraction that is associated to the direction of the load.

From the previous works [43, 44], the E-modulus has been raised by increased stress with a mean value of 81.2 MPa. Tensile tests were conducted independently for Z-HDPE composites, with the average E-modulus of 1.8 GPa within SF to Z-HDPE weight ratios of 5.95. Figure 6 shows an E-modulus, which is determined in relation to the SF orientation. The theoretical E-modulus is generally 15-20% higher than the experimental value.

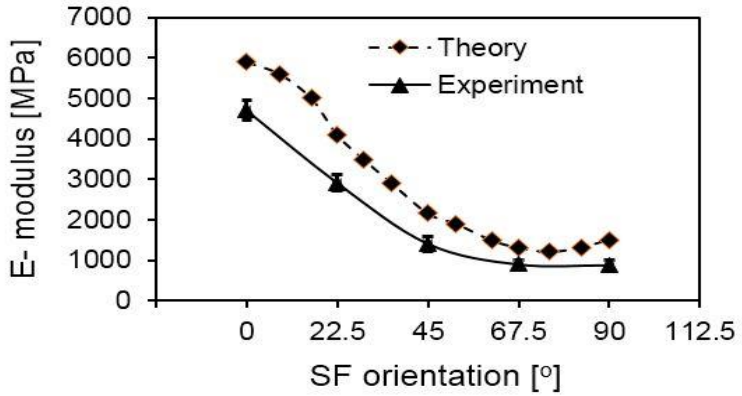

Fig. 8. The E-modules focused in various SF configurations on theoretical and experimental.

3.3. Tensile fracture morphologies

Surface morphology depicted by SEM as shown in Fig. 9 is focused on 0° SF. Figure 9(a) indicates that the SF is not broken but separated from a half-shattered side plane. Many voids are removed around both the fiber and particles. Also, Fig. 9(a) shows

the presence of plastically deformed ligaments that indicated a ductile fracture for the specimen in a yellow rectangle. In the HDPE matrix, the appearance of troughs on the broken surface (white rings, as shown in Fig. 9(b) effects the removal of the fibers during the stress test. This is not a new trend and is still evident in several studies, considering its use of fiber from different materials [45, 46].

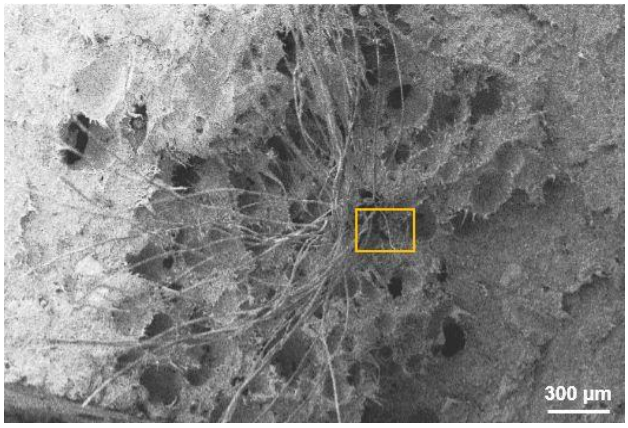

(a) Fractures in the midst of thickness indicating the void's existence and the zeolite pulled out.

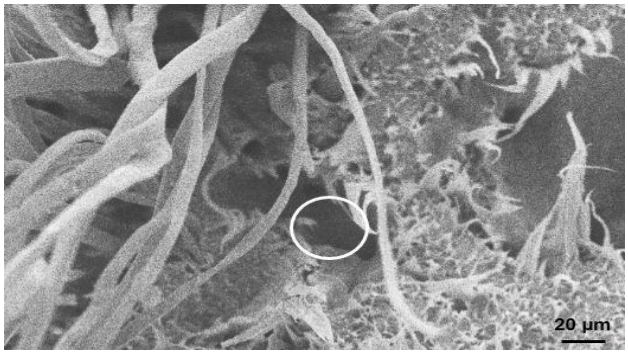

(b) Enhancement of the yellow rectangle zone shown in Fig. 8(a).

Fig. 9. The SEM analysis on tensile fracture surface of composites.

On the surface of the composite's tensile fractures, ligaments with a direction other than 0° were also seen, Figs. 10(a) and (b). The fibers which come out of a fracture are not perpendicular to the main plane. This symptom also occurs in composites which the fiber was organized in tensile load direction. Energy is consumed in composites with different fiber orientations for work under various fiber extraction mechanisms and composite fracture work.

Many voids, pores that are not filled with polymers, particles and fibers, were found in the material being examined. Such voids are undesirable and are primarily the consequence of poor material. The tensile strength of composites can be impaired by these voids [47-50].

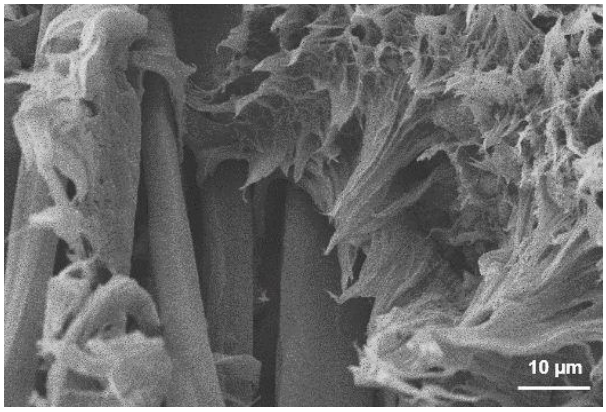

(a) Enhancement of the yellow rectangle zone shown.

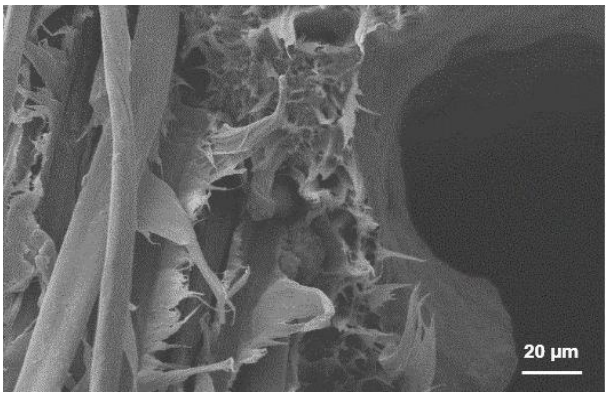

(b) Enhancement of the yellow rectangle.

Fig. 10. The surface fracture test for composite with 22,5° SF orientation.

4. Conclusions

The mechanical performance of Z/HDPE composites reinforced SF in various orientations was evaluated. Material properties strongly depend on the SF orientation. At an SF position of 0o, the SF strengthening effect on mechanical performance was the strongest. It is noticeable that fibers should be placed in parallel to the longitudinal direction to achieve good tensile strength and flexural strength. In order to increase mechanical strength, particularly the flexural and tensile properties, the fibers should not be placed across the board, as both of them have the lowest properties.

For each additional 22.5° fiber orientation angle, flexural strength and breaking energy decreased by about 10%. The addition of the fiber orientation angle, on the other hand, irregularly reduces the flexural modulus and other tensile properties. Moreover, the theoretical E-modulus value is 15 to 20% greater than that of the experimental value. At the SF 90° orientation, cos4θ is equal to zero; thus, the fiber does not make the material rigid. This information is beneficial for material load design.

There is future work to explore the fracture and tensile properties of SF-Z/HDPE composite in consequence of the introduction of coupling agent materials from trimethyl-methoxy silane. Furthermore, in order to increase the crystallinity of the matrix, pressure treatment is designed to create a composite with an adjustable fiber orientation that has a strong adhesion strength.

Acknowledgement

This study was financially supported by the Ministry of Research and Technology/National Research and Innovation Agency of Republic Indonesia (Kementerian Riset dan Teknologi/Badan Riset dan Inovasi Nasional).

Nomenclatures

E_c	Modulus of composite
E_f	E-modulus of fiber
E_m	E-modulus of matrix
L	Composites length
t	Composites width
V_f	Volume fraction of fibers
V_m	Volume fraction of matrix

Greek Symbols

α_n	fiber fraction associated to the direction of the load
β	Silk fiber angle
θ	Direction of load to fiber orientation
η_0	Parameters modified for fiber ratio
η_1	Parameters modified for fiber length distribution
η_d	Parameters modified for fiber diameter distribution

Abbreviations

ASTM	American Society for Testing and Materials
HDPE	High-Density Polyethylene
ISO	International Organization for Standardization
SEM	Scanning electron microscopy
SF	Silk Fiber
Z	Zeolite

References

1. Kandemir. A.; Pozegic, T.R.; Hamerton, I.; Eichhorn, S.J.; and Longana, M.L. (2020). Characterisation of natural fibres for sustainable discontinuous fibre composite materials. *Materials*, 13(2129), 1-17.
2. Longana, M.L.; Ondra, V.; Yu, H.; Potter, K.D.; and Hamerton, I. (2018). Reclaimed carbon and flax fibre composites: manufacturing and mechanical properties. *Recycling*, 3(52), 1-13.
3. Wang, F.; Lu, M.; Zhou, S.; Lu, Z.; and Ran, S. (2019). Effect of fiber surface modification on the interfacial adhesion and thermo-mechanical performance

of unidirectional epoxy-based composites reinforced with bamboo fibers. *Molecules*. 24(15), 2682.

4. Ouajai, S.; and Shanks, R.A. (2005). Composition, structure and thermal degradation of hemp cellulose after chemical treatments. *Polymer Degradation and Stability*, 89(2), 327-335.
5. Yu, H.; Longana, M.L.; Jalalvand, M.; Wisnom, M.R.; and Potter, K.D. (2017). Hierarchical pseudo-ductile hybrid composites combining continuous and highly aligned discontinuous fibres. *Composites Part A: Applied Science and Manufacturing*, 105, 40-56.
6. Gunti, R.; Prasad, A.V.R.; and Gupta, A.V.S.S.K.S. (2018). Mechanical and degradation properties of natural fiber-reinforced PLA composites: jute, sisal, and elephant grass. *Polymer Composites*, 39(4), 1125-1136.
7. Rajak, D.K.; Pagar, D.D.; Menezes, P.L.; and Linul, E. (2019). Fiber-reinforced polymer composites: manufacturing, properties, and applications. *Polymers*, 11(10), 1667.
8. Dicker, M.P.M.; Duckworth, P.F.; Baker, A.B. (2014). Green composites: a review of material attributes and complementary applications. *Composites Part A: Applied Science and Manufacturing*, 56, 280-289.
9. Constante, A.; and Pillay, S. (2018). Compression moulding of algae fiber and epoxy composites: modeling of elastic modulus. *Journal of Reinforced Plastics and Composites*, 37(19), 1202-1216.
10. Sormunen, P.; and Kärki, T. (2019). Compression molded thermoplastic composites entirely made of recycled materials. *Sustainability*, 11(3), 631.
11. Idicula, M.; Sreekumar, P.A.; Joseph, K.; and Thomas, S. (2009). Natural fiber hybrid composites - a comparison between compression moulding and resin transfer moulding. *Polymer Composites*, 30(10), 1417-1425.
12. Zampaloni, M.; Pourboghrat, F.; Yankovich, S.A.; Rodgers, B.N.; Moore, J.; Drzal, L.T.; Mohanty, A.K.; and Misra, M. (2007). Kenaf natural fiber reinforced polypropylene composites: a discussion on manufacturing problems and solutions. *Composites Part A: Applied Science and Manufacturing*, 38(6), 1569-1580.
13. Andersson, M.; Johansson, J.; and Rising, A. (2016). Silk spinning in silkworms and spiders. *International Journal of Molecular Sciences*, 17(8), 1290.
14. Kronqvist, N.; Otikovs, M; Chmyrov, V.; Chen, G.; Andersson, M.; Nordling, K.; and Widengren, J. (2014). Sequential Ph-driven dimerization and stabilization of the n-terminal domain enables rapid spider silk formation. *Nature Communications*, 5(1), 3254.
15. Johari, N.; Moroni, L.; and Samadikuchaksaraei, A. (2020). Tuning the conformation and mechanical properties of silk fibroin hydrogels. *European Polymer Journal*, 134, 109842.
16. Mohammadzadehmoghadam, S.; and Dong, Y. (2019). Fabrication and characterization of electrospun silk fibroin/gelatin scaffolds crosslinked with glutaraldehyde vapor. *Frontiers in Materials*, 6, 1-12.
17. Ataollahi, S.; Taher, S.T.; Eshkoor, R.A.; Arifn, A.K.; Azhari, C.H. (2012). Energy absorption and failure response of silk/epoxy composite square tubes: experimental. *Composites Part B: Engineering*, 43(2), 542-548.

18. Ude, A.U.; Arifn, A.K.; and Azhari, C.H. (2013). Impact damage characteristics in reinforced woven natural silk/epoxy composite face-sheet and sandwich foam, coremat and honeycomb materials. *International Journal of Impact Engineering*, 58, 31–38.
19. Hamidi, Y.K.; Yalcinkaya, M.A.; Guloglu, G.E.; Pishvar, M.; Amirkhosravi, M.; and Altan, M.C. (2018). Silk as a natural reinforcement: processing and properties of silk/epoxy composite laminates. *Materials*, 11, 2135.
20. Yang, Y.; Zhao, D.; Xu, J.; Dong, Y.; Ma, Y.; Qin, X.; Fujiwara, K.; Suzuki, E.; Furukawa, T.; Takai, Y.; and Hamada, H. (2018). Mechanical and optical properties of silk fabric/glass fiber mat composites: an artistic application of composites. *Textile Research Journal*, 88(8), 932-945.
21. Saleem, M.; Rasheed, S.; and Yougen, C. (2020). Silk fibroin/hydroxyapatite scaffold: a highly compatible material for bone regeneration. *Science and Technology of Advanced Materials*, 21(1), 242-266.
22. Farokhi, M.; Mottaghitalab, F.; Samani, S.; Shokrgozar, M.A.; Kundu, S.C.; Reis, R.L.; Fatahi, Y.; and Kaplan, D.L. (2018). Silk fibroin/hydroxyapatite composites for bone tissue engineering. *Biotechnology Advances*, 36(1), 68-91.
23. Moses, J.C.; Nandi, S.K.; and Mandal, B.B. (2018). Multifunctional cell instructive silk-bioactive glass composite reinforced scaffolds toward osteoinductive, proangiogenic, and resorbable bone grafts. *Advanced Healthcare Materials*, 7(10), 1701418.
24. Wu, J.; Zheng, K.; Huang, X., Liu, J.; Liu, H.; Boccaccini, A.R.; Wan, Y.; Guo, X.; and Shao, Z. (2019). Thermally triggered injectable chitosan/silk fibroin/bioactive glass nanoparticle hydrogels for in-situ bone formation in rat calvarial bone defects. *Acta Biomaterialia*, 91, 60-71.
25. Midha, S.; Kumar, S.; Sharma, A.; Kaur, K.; Shi, X.; Naruphontjirakul, P.; Jones, J.R.; Ghosh, S. (2018). Silk fibroin-bioactive glass based advanced biomaterials: towards patient-specific bone grafts. *Biomedical Materials*, 13(5), 055012.
26. Purnomo; and Subri, M. (2017). Post-yield fracture behavior of zeolite-reinforced high density polyethylene annealed composite. *International Review of Mechanical Engineering*, 11(1), 87-93.
27. Purnomo; Soenoko, R.; Irawan, Y.S.; and Suprapto, A. (2017). Deformation under quasi static loading in high density polyethylene filled with natural zeolite. *Journal of Engineering Science and Technology*, 12(5), 1191-1203.
28. Purnomo; Subri, M; and Setyarini, P.H. (2018). Fracture development and deformation behavior of zeolite-filled high density polyethylene annealed composites in the plane stress fracture. *FME Transactions*, 46, 165-170.
29. Purnomo; and Setyarini, P.H. (2018). Atmospheric-pressure annealing effect on the impact fracture toughness of injection-molded zeolite-hdpe composite. *International Review of Mechanical Engineering*, 12(6), 556-562.
30. Vinod, B.; and Sudev, L.J. (2013). Effect of fiber orientation on the flexural properties of palf reinforced bisphenol composites. *International Journal of Science and Engineering Applications*, 2(8), 166-169.
31. Canché-Escamilla G.; Rodriguez-Laviada J.; Cauich-Cupul, J.I.; Mendizábal, E.; Puig, J.E.; and Herrera-Franco, P.J. (2002). Flexural, impact and compressive properties of a rigid-thermoplastic matrix/cellulose fiber

reinforced composites. *Composites Part A: Applied Science and Manufacturing*, 33(4), 539-549.

32. Turkaslan, S.; Tezvergil-Mutluay, A.; Bagis, B; Pekka, K.; Vallittu. P.K.; and Lassila, V.J. (2009). Effect of fiber-reinforced composites on the failure load and failure mode of composite veneers. *Dental Materials*, 28(5). 530-536.
33. Mosharraf, R; and Givechian, P. (2012). Effect of Fiber Position and Orientation on Flexural Strength of Fiber-Reinforced Composite. *Journal of Islamic Dental Association of IRAN* (*JIDAI*), 24(2), 21-27.
34. vanHeumen, C.C.; Kreulen, C.M.; Bronkhorst, E.M.; Lesaffre, E.; and Creugers, N.H. (2008). Fiber-reinforced dental composites in beam testing. *Dental Materials*, 24(11),1435-1443.
35. Kuboki, T. (2014). Foaming behavior of cellulose fiber-reinforced polypropylene composites in extrusion. *Journal of Cellular Plastics*, 50(2), 113–128
36. Irfan, M.S.; Saeed, F.; Gill, Y.Q.; and Qaiser, A.A. (2018). Effects of hybridization and fiber orientation on flexural properties of hybrid short glass fiber and short carbon fiber-reinforced vinyl ester composites. *Polymers and Polymer Composites*, 26(5-6), 371-379.
37. YuK, H.; Potter, D.; and Wisnom, M.R. (2014). A novel manufacturing method for aligned discontinuous fiber composites (high performance-discontinuous fiber method). *Composites Part A: Applied Science and Manufacturing*, 65, 175-185.
38. Mortazavian, S.; and Fatemi, A. (2015). Effects of fiber orientation and anisotropy on tensile strength and elastic modulus of short fiber reinforced polymer composites. *Composites Part B: Engineering*, 72, 116-129.
39. Goldberg, O.; Greenfeld, I.; and Wagner, H.D. (2020). Efficient toughening of short-fiber composites using weak magnetic fields. *Materials* (*Basel*), 13(10), 2415.
40. Virk, A.; Hall, W.; and Summerscales, J. (2012). Modulus and strength prediction for natural fiber composites. *Materials Science and Technology*, 28(7), 864-871.
41. Cordin, M.; Bechtold, T.; and Pham, T. (2018). Effect of fiber orientation on the mechanical properties of polypropylene-lyocell composites. *Cellulose*, 25(12), 7197-7210.
42. Krenchel, H. (1964). Fibre reinforcement: theoretical and practical investigations of the elasticity and strength of fibre-reinforced materials. Copenhagen, Akademisk Forlag.
43. Mazumder, M.R.H.; Numera, F.; Al-Asif, A.; and Hasan, M. (2018). Mechanical properties of silk and glass fiber reinforced hybrid polypropylene composites. *IOP Conference Series: Materials Science and Engineering*, 438, 012007
44. Zhang, K.; Si, F.W.; Duan, H.L.; and Wang J. (2010). Microstructures and mechanical properties of silks of silkworm and honeybee. *Acta Biomaterialia*, 6(6), 2165-2171.
45. Huang, Y.; Fei, B.; and Zhao, C. (2016). Mechanical properties of bamboo fiber cell walls during the culm development by nanoindentation. *Industrial Crops and Products*, 92, 102-108.

46. Fuentes, C.A.; Brughmans, G.; Tran, L.Q.N.; Dupont-Gillain, C.; Verpoest, I.; and Van Vuure, A.W. (2015). Mechanical behavior and practical adhesion at a bamboo composite interface: Physical adhesion and mechanical interlocking. *Composites Science and Technology*, 109, 40-47.
47. Mehdikhani, M.; Gorbatikh, L.; Verpoest, I.; and Lomov, S.V. (2018). Voids in fiber-reinforced polymer composites: a review on their formation, characteristics, and effects on mechanical performance. *Journal of Composite Materials*, 53(12), 1579-1669.
48. Zakaria, K. Z.; Akil, H.M.; Shamsuddin, M.S.M.; and Mohd Ishak, Z.A. (2020). Mechanical performance of pultruded kenaf/glass hybrid fiber reinforced unsaturated polyester under hygrothermal conditions. *AIP Conference Proceedings*, 2267, 020045.
49. Bodaghi, M.; Cristóvão, C.; and Gomes, R. (2016). Experimental characterization of voids in high fiber volume fraction composites processed by high injection pressure RTM. *Composites Part A: Applied Science and Manufacturing*, 82, 88-99.
50. Neuenschwander, J.; Furrer, R.; and Roemmeler, A. (2016). Application of air-coupled ultrasonics for the characterization of polymer and polymer-matrix composite samples. *Polymer Testing*, 56, 379-386.